

REPORT DOCUMENTATION PAGE			Form Approved OMB NO. 0704-0188		
<p>The public reporting burden for this collection of information is estimated to average 1 hour per response, including the time for reviewing instructions, searching existing data sources, gathering and maintaining the data needed, and completing and reviewing the collection of information. Send comments regarding this burden estimate or any other aspect of this collection of information, including suggestions for reducing this burden, to Washington Headquarters Services, Directorate for Information Operations and Reports, 1215 Jefferson Davis Highway, Suite 1204, Arlington VA, 22202-4302. Respondents should be aware that notwithstanding any other provision of law, no person shall be subject to any penalty for failing to comply with a collection of information if it does not display a currently valid OMB control number.</p> <p>PLEASE DO NOT RETURN YOUR FORM TO THE ABOVE ADDRESS.</p>					
1. REPORT DATE (DD-MM-YYYY) 16-07-2009		2. REPORT TYPE Final Report		3. DATES COVERED (From - To) 5-Aug-2004 - 30-Nov-2008	
4. TITLE AND SUBTITLE Solid State Quantum Computing using Spin Qubits in Silicon Quantum Dots (QCCM)			5a. CONTRACT NUMBER W911NF-04-1-0389		
			5b. GRANT NUMBER		
			5c. PROGRAM ELEMENT NUMBER		
6. AUTHORS Mark Eriksson, Max Lagally, Mark Friesen, Susan Coppersmith, Robert Joynt, Robert Blick, Alex Rimberg, Stephen Lyon, Paul von Allmen, Gerhard Klimeck			5d. PROJECT NUMBER		
			5e. WORK NUMBER <del>611102</del>		
			5f. WORK UNIT NUMBER <del>611102</del>		
7. PERFORMING ORGANIZATION NAMES AND ADDRESSES University of Wisconsin - Madison The Board of Regents of the UW System 21 N. Park Street Madison, WI 53715 -1218			8. PERFORMING ORGANIZATION REPORT NUMBER		
9. SPONSORING/MONITORING AGENCY NAME(S) AND ADDRESS(ES) U.S. Army Research Office P.O. Box 12211 Research Triangle Park, NC 27709-2211			10. SPONSOR/MONITOR'S ACRONYM(S) ARO		
			11. SPONSOR/MONITOR'S REPORT NUMBER(S) 46260-PH-OC.67		
12. DISTRIBUTION AVAILABILITY STATEMENT Approved for public release; Distribution Unlimited					
13. SUPPLEMENTARY NOTES The views, opinions and/or findings contained in this report are those of the author(s) and should not construed as an official Department of the Army position, policy or decision, unless so designated by other documentation.					
14. ABSTRACT The project goals are to fabricate qubits in quantum dots in Si/SiGe modulation-doped heterostructures, to characterize and understand those structures, and to develop the technology necessary for a Si/SiGe quantum dot quantum computer. The physical qubit in our approach is the spin of an electron confined in a top-gated silicon quantum dot in a Si/SiGe modulation-doped heterostructure. Operations on such a qubit may be performed by controlling the voltages on gates in-between neighboring quantum dots. A quantum computer and qubits in silicon					
15. SUBJECT TERMS quantum computing, qubits, silicon devices, quantum dots, spins, valley splitting, quantum point contact, decoherence, single electron transistor, spin blockade					
16. SECURITY CLASSIFICATION OF:			17. LIMITATION OF ABSTRACT SAR	15. NUMBER OF PAGES	19a. NAME OF RESPONSIBLE PERSON Mark Eriksson
a. REPORT U	b. ABSTRACT U	c. THIS PAGE U			19b. TELEPHONE NUMBER 608-262-2281

## 2004-2008 UW QCCM Final Report

### Table of Contents:

<b>Statement of the problem studied</b>	<b>1</b>
<b>Summary of the most important results:</b>	
<b>University of Wisconsin-Madison</b>	<b>2</b>
<b>Dartmouth College</b>	<b>8</b>
<b>Princeton University</b>	<b>10</b>
<b>JPL and Purdue University</b>	<b>13</b>
<b>Bibliography</b>	<b>17</b>

### **Statement of the Problem Studied:**

The project goals are to fabricate qubits in quantum dots in Si/SiGe modulation-doped heterostructures, to characterize and understand those structures, and to develop the technology necessary for a Si/SiGe quantum dot quantum computer.

### **Project Overview:**

The physical qubit in our approach is the spin of an electron confined in a top-gated silicon quantum dot in a Si/SiGe modulation-doped heterostructure.[1-3] Operations on such a qubit may be performed by controlling the voltages on gates in-between neighboring quantum dots.[4] A quantum computer and qubits in silicon offer potential advantages, both fundamental and practical. Electron spins in silicon quantum dots are expected to have long coherence times. Silicon has an isotope,  $^{28}\text{Si}$ , which has zero nuclear spin and thus no nuclear magnetic moment. As a result, electron spins in silicon have longer coherence times than they would in the presence of a fluctuating nuclear spin background. From a practical perspective, modern classical computers are made in silicon, and one hopes that this will lead to synergy in the future with a silicon quantum computer. This QCCM includes both theory and experiment focusing on (i) the development of qubits in the form of electron spins in silicon quantum dots, (ii) the measurement and manipulation of those qubits, and (iii) the science essential for understanding the properties of such qubits.

**A. Work led by Wisconsin (M. A. Eriksson, S. N. Coppersmith, R. Joynt, M. Friesen, R. Blick, M. G. Lagally).**

***Summary of Major Accomplishments During Grant Period:***

1. Achievement of single-electron quantum dots with integrated charge sensing.
2. Demonstration of charge sensing in a Si/SiGe double quantum dot.
3. Demonstration of spin-to-charge conversion in the form of spin blockade in a Si/SiGe double quantum dot.
4. Observation and characterization of strongly energy-dependent loading of Si/SiGe quantum dot.
5. Application of pulsed-gate voltages to quantum dot.
6. Characterization and elucidation of valley splitting in SiGe heterostructures and devices.
7. Improvement of SiGe heterostructures.
8. Development of low-leakage top gates for quantum dots in SiGe.
9. Improved theoretical understanding of singlet-triplet relaxation.
10. Improved theoretical understanding of valley mixing and effect on gate operations.

**Discussion of Major Accomplishments:**

**1. Achievement of single-electron quantum dots with integrated charge sensing.**

We performed charge sensing measurements in single quantum dots and demonstrated strong evidence of a one-electron dot in Si/SiGe.[5] As shown in Fig. 1, we have been able to tune a quantum dot into a regime in which we can see a very large region with no charge transitions.

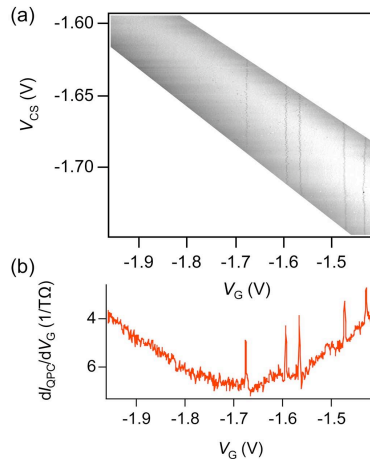


**Fig. 1** Charge sensing showing the last five transitions out of a quantum dot. (a) Gray-scale plot of the current through the charge-sensing quantum point contact. No further transitions occur for  $V_G < -1.68$  V, indicating that the quantum dot is empty of electrons in this regime. (b) An average of 7 line-cuts taken diagonally down the sensitive slice in part (a). The sharp peaks correspond to changes in the electron occupation of the dot. (Adapted from Ref. 5.)

## 2. Demonstration of charge sensing in a Si/SiGe double quantum dot.

We demonstrated charge-sensing measurements in a Si/SiGe double quantum dot, as shown in Fig. 2. This is an important advance, because charge sensing in such a double dot is one of the key elements required for measurement of coherence times in semiconductor quantum dots. The data in Fig. 2 show an asymmetry in the charge transitions, indicating that one quantum dot is likely larger than the other, and thus at least one of the quantum dots for this data was not in the few-electron regime.

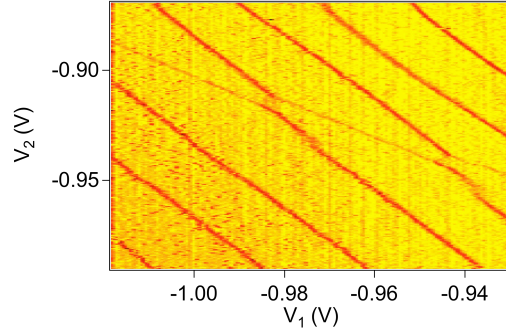


**Fig. 2** Charge sensing in a double quantum dot.

## 3. Demonstration of spin-to-charge conversion in the form of spin blockade in a Si/SiGe double quantum dot.

Spin blockade is the canonical example of spin-to-charge conversion in transport, where charge current is blocked in a double quantum dot by a metastable spin state (Fig. 3). Spin blockade is important, because it is the basis of a number of recent advances in spintronics, including the measurement and the manipulation of individual electron spins.[6, 7]

Experimentally, we observe spin blockade as shown in Fig. 3a-c. These measurements are taken at finite bias voltage across the dot, where current flows in regions commonly called “bias triangles.” When T(1,1) is loaded and no relaxation occurs from T(1,1) to S(1,1), spin blockade is observed (as marked by the orange triangle), and the bias triangle is truncated as shown schematically in Fig. 3b. Spin blockade is fully lifted when the T(2,0) state is brought below the T(1,1) state (blue star). We now have shown that this aspect of spin blockade in Si is virtually identical to that previously observed in other systems.[8]

## 4. Observation and characterization of strongly energy-dependent loading of Si/SiGe quantum dot.

We have also made an important discovery about tunneling in Si/SiGe quantum dots. Tunneling rates in and out of quantum dots can be quite sensitive to the electrostatic barrier between the dot and the leads. Such tunneling is an excellent example of tunneling through a finite height barrier, and it has a well-known exponential dependence on barrier height. In principle, the fact that electrons have a relatively large

effective mass in Si,  $m^* = 0.19 m_e$ , means that the dependence on barrier height should be stronger in silicon than in materials with a lighter effective mass. Our data for Si/SiGe double quantum dots does indeed seem to show this strong dependence,[8] and it is revealed by what is called energy-dependent-tunneling in the double dot literature. This effect demonstrates that silicon is interesting not only for its low

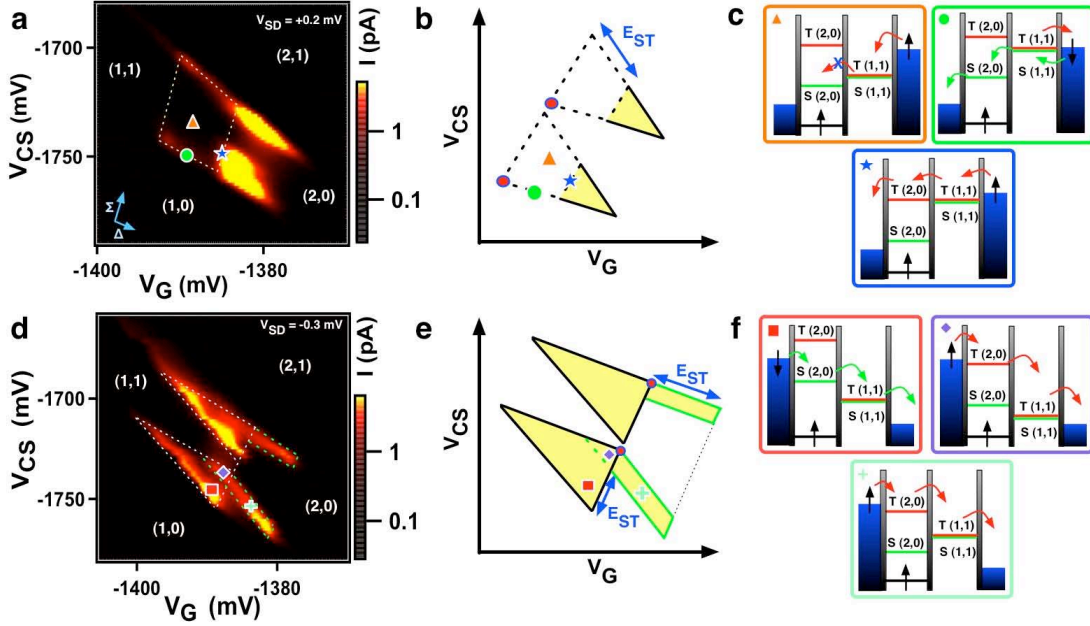


**Fig. 3** Spin blockade and lifetime-enhanced transport (Ref. 8):

(a) Positive bias ( $V_{SD} = 0.2$  mV) triangles representing the (1,0)-(1,1)-(2,0)-(2,1) charge transition. Current through the device is blocked due to Pauli spin blockade (as marked by the orange triangle) in the region outlined by yellow dashed lines. (b) Schematic representation of the positive bias triangles. (c) Transport details and energy level schematics for the electron triangle corresponding to the points denoted by the green circle, orange triangle, and blue star in (a) and (b).

(d) Negative bias ( $V_{SD} = -0.3$  mV) triangles through the same charge transition. Current flow through full electron and hole triangles (white dashed lines) is observed. In addition, strong ‘tails’ of current (green dashed parallelograms) are observed at the base of the triangles. These extensions arise due to LET. (e) Schematic representation of the negative bias triangles. Regions outlined by the solid back lines correspond to conventional electron transport, while those outlined by solid green lines (the tails) correspond to LET. (f) Transport details and energy level schematics for the electron triangle corresponding to the points denoted by the red square, purple diamond and teal cross in (d) and (e).

spin-orbit coupling and its zero-spin nuclear isotopes, but further the relatively large effective mass can also be useful, once one learns to design quantum dots to take advantage of this effect.

## 5. Application of pulsed-gate voltages to a quantum dot.

We have also demonstrated a second key element for coherence time measurements: the ability to apply pulsed gate voltages and measure its effect on the electronic state of a single quantum dot, as shown in

Fig. 4. The next step in this effort is to combine charge sensing with pulsed gate voltages and single electron occupation, each of which we have now demonstrated separately.

### **6. Characterization and elucidation of valley splitting in Si/SiGe heterostructures and devices.**

Silicon is an indirect band-gap semiconductor, a property that results in two valley states that are potentially important in quantum dots. In principle, these valleys can double the number of quantum states in a qubit. We have performed experiments in silicon quantum point

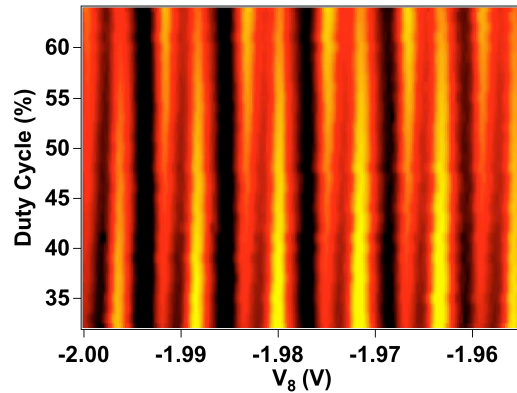


**Fig. 4** Coulomb blockade peaks measured during the application of a pulsed gate voltage, resulting in a doubling of the number of peaks. As the duty cycle changes, the weight shifts from one of the doubled peaks to the other. At 50% duty cycle, the weight is not evenly split between the two peaks, which may be due to an asymmetric peak shape, or may have a more interesting explanation, something we are currently investigating.

contacts showing that the valley splitting can be quite large in such laterally confined devices.[9] We have also developed a good theoretical understanding of this effect. The valley splitting arises due to both vertical confinement in the quantum well and lateral confinement in the quantum point contact. Similar confinement occurs in quantum dots. The controlled confinement provides a mechanism to make valley splitting large, simplifying the low-lying quantum states in a silicon quantum dot qubit.

### **7. & 8. Improvement of SiGe heterostructures and development of low-leakage top gates for quantum dots in SiGe.**

We have made improvements in our quantum well growth, achieving mobility over 100,000 cm<sup>2</sup>/Vs in samples that also have the correct doping profile for gateability. Advances in materials and fabrication processes have been crucial for all the experimental advances reported here.

### **9. Improved theoretical understanding of singlet-triplet relaxation.**

In June of 2008 we published the first observation of lifetime-enhanced transport (LET).[8] This was a major step for us, as it is an example of the discovery of novel quantum dot physics in Si/SiGe, and thus illustrates the large improvements in quality that have been made in such dots over the last several years.

One part of that publication was the report of  $16 \mu\text{s}$  as a lower bound on the triplet-singlet relaxation time. As we discuss here, from theory we expect this relaxation time to be much longer than this first bound, but the  $16 \mu\text{s}$  time is still an important step because it is the first spin relaxation bound available for Si/SiGe quantum dots.

We performed a theoretical investigation of singlet-triplet relaxation in a two-electron silicon quantum dot. In the absence of a perpendicular magnetic field, we find that spin-orbit coupling is not the main source of singlet-triplet relaxation. Instead, relaxation in this regime occurs mainly via virtual states and is due to nuclear hyperfine coupling. In addition, we find that, in an external magnetic field perpendicular to the plane of the dot, spin-orbit coupling plays a particularly important role for decoherence. Indeed, a strong anisotropy emerges: parallel magnetic field can increase substantially the relaxation time due to Zeeman splitting, but when the magnetic field is applied perpendicular to the plane, the enhancement of the spin-orbit effect shortens the relaxation time. This relaxation is found to be orders of magnitude slower than for GaAs quantum dots, due to weaker hyperfine and spin-orbit effects in that system. Our calculations are consistent with the observed lower bound for singlet-triplet relaxation, described above, although a stronger bound on the decoherence rate will provide additional insight.

### 10. Improved theoretical understanding of valley mixing and effect on gate operations.

We have also modeled data for transport through Si/SiGe quantum point contacts and identified valley splitting in magnetic subbands. We have shown that valley splitting can be suppressed when electronic wavefunctions cover many steps at the quantum well interface.[10] The suppression can be controlled by confining the wavefunctions, laterally, to reduce the

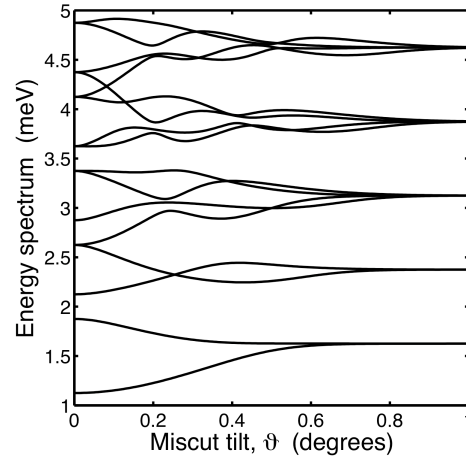


**Fig. 5** Theoretical calculations of valley-coupled orbitals in an elliptical quantum dot grown on a tilted substrate. For large miscuts, the valley splitting is suppressed when an electron covers many steps at the quantum well interface. Note that each pair of states exhibits a valley splitting. In addition, inter-orbital valley couplings are observed as anti-crossings and asymmetries in the energy spectrum.

number of steps covered. We have developed a theory for QPCs, taking into account the fact that wavefunctions in different magnetic subbands have different shapes, and should therefore exhibit different valley splittings. We used QPC spectroscopy to analyze the valley splitting in different subbands.

A similar physical picture applies to quantum dots: excited orbitals cover more steps, leading to a suppressed valley splitting. In addition, a typical dot energy spectrum displays valley couplings that involve many orbitals, as shown in Fig. 5. Theoretical results show that the ground state valley splitting is sufficient for the purposes of quantum computing, for a physically reasonable quantum dot radius that depends on the local tilt angle of the interface. For typical miscut angles and a physically realistic dot radius, the characteristic exchange coupling is of order  $2 \mu\text{eV}$ , corresponding to a SWAP gate times of order 1 ns. This is well within the desired range for quantum computing.



## B. Work led by Dartmouth (A. Rimberg).

### Fabrication of RF-SETs integrated with Si/SiGe quantum dots:

During the final funding period of the grant there was continued progress at Dartmouth in producing Si/SiGe quantum dots (QD) for eventual coupling to a radio-frequency single-electron transistor (RF-SET). By using a combination of deeper etching and backfilling with  $\text{Al}_2\text{O}_3$ , as shown in Fig. 6(a) and (b), Alex Rimberg's group has successfully produced structures with low-leakage Schottky gates entirely at Dartmouth. In these structures, typical leakage currents are held to less than a few

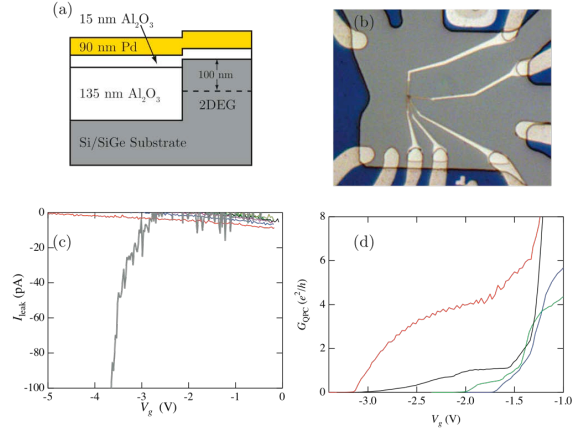


**Fig. 6** (a) Fabrication scheme for low-leakage gates, including deep etch and oxide backfill. (b) Micrograph of a typical mesa fabricated using this new scheme. (c) Leakage currents for low-leakage gates are usually sub pA to voltages of negative 3 V. (d) Typical QPC pinchoff.

pA, to voltages of at least negative 3 V, as shown in Fig. 6(c). Yield for this process is extremely high (essentially 100% of gates show performance as in Fig. 6(c)) which is essential for eventual coupling of Si/SiGe QDs to SETs. Using this new fabrication technique has allowed the Rimberg group to routinely produce quantum point contact with clean, reproducible and stable pinchoff, as shown in Fig. 6(d).

Preliminary measurements on Si/SiGe QD structure with a standard few-electron gate structure have yielded very encouraging results, as shown in Fig. 7 (a). Here we show a set of Coulomb blockade oscillations as captured using a digital oscilloscope. Three clearly defined current peaks are visible versus the applied gate voltage. The dot that caused these oscillations was not particularly stable, hence the need to do a rapid measurement of Coulomb blockade. This instability is presumably due in part to the large electric fields associated with the relatively high pinchoff voltages on the order of negative 2 to 3 V shown in Fig. 6(d). We have very recently begun to fabricate devices using Si/SiGe material with lower electron sheet density, resulting in a roughly five-fold reduction in pinchoff voltage, as in Fig. 7(b)

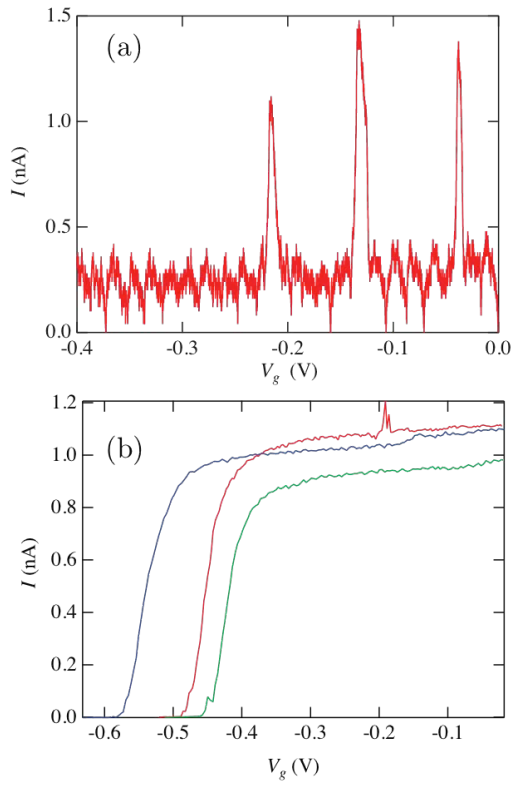


**Fig. 7** (a) Coulomb blockade oscillations for a few-electron Si/SiGe QD. (b) Low-voltage pinchoff data.

### **C. Work led by Princeton (S. Lyon)**

#### **Electron Spin Coherence in Si/SiGe Quantum Structures:**

While electrons bound to phosphorus donors in Si have been shown to have extremely long  $T_2$ 's (approaching a second), there is no direct experimental evidence that electron spins have similarly long coherence times in Si quantum dots. The goal of this research has been to understand what controls the spin coherence of an electron bound in a Si dot, and to discover how Si quantum dots must be designed and fabricated in order to obtain long spin coherence.

We began this project by measuring the spin relaxation of Si-dots that had previously been fabricated at the University of Wisconsin-Madison. The dots were made by first growing a modulation-doped Si quantum well embedded in SiGe. Electron-beam lithography was then used to define the dots, and the quantum well was etched away from the surrounding areas. The smallest dots were about 400nm in diameter, and we measured their spin coherence to be essentially the same as in the unpatterned quantum wells. While we measured coherence times,  $T_2$ , of about a microsecond, we did not find an effect of the confinement. In particular, the  $T_2$  time did not increase significantly at lower temperature (down to 2K). There are two likely explanations for the “short” spin coherence in these large dots: first that the extra states arising from the nearly degenerate conduction band valleys were decohering the electron spins; or second, that the dots were too big, thus requiring too low a temperature to obtain long spin coherence.

To investigate the effect of a valley degeneracy, we have measured the relaxation of electron spins bound to lithium donors in Si. Unlike all other shallow donors in Si, the ground state of Si:Li is valley degenerate. We found that the spin relaxation is faster than our time resolution ( $<100\text{ns}$ ) in  $^{28}\text{Si:Li}$ . However, if the crystal is purposely strained, breaking the valley degeneracy, we measured much longer spin coherence times ( $> 10\mu\text{s}$  at 2K). This is direct experimental evidence that valley degeneracies must be lifted for long spin coherence in Si.

We first addressed the issue of fabricating smaller quantum dots by patterning Si/SiGe quantum wells using nanoimprint lithography, reactive ion etching (RIE) and a selective wet chemical etch. There was concern, initially, that RIE would introduce too much damage and all the electrons in the dots would

be trapped by the defects. Immediately after the RIE step we see a large signal from defects, but a short wet chemical etch removes the defects and we see signals associated with the undamaged quantum well.

While nanoimprint lithography can rapidly pattern dots over large areas, it introduces some problems. First, the surface of the Si/SiGe samples is not perfectly flat, with a small corrugation on a few micron lateral scale. The nanoimprint mold cannot follow these variations in the surface topography, and thus there is a modulation in the size of the dots across the sample. In addition, nanoimprint lithography requires a using relatively large area (at least  $\sim 4 \text{ cm}^2$ ), since there are a few mm around the edge where the mold does not make good contact. Thus this method of patterning quantum dots is wasteful of Si/SiGe material. To alleviate these problems we have found a way to write quantum dot patterns over large areas with a new electron beam (ebeam) lithography tool. In the usual approach, one programs the ebeam system to write each dot. This approach is prohibitively slow for the large numbers of dots that we need to obtain a useful signal. Instead, we have found that we can program the ebeam to simply write a line, but then adjust the number of spots/ $\mu\text{m}$  to give a series of dots. Furthermore, the size of the exposed dot can be reliably controlled by adjusting the electron beam current. While slower than nanoimprint lithography the added flexibility and insensitivity to surface profile are significant advantages of the electron beam patterning. Our system can pattern dots with a density of over  $10^9/\text{cm}^2$  at a throughput of a few  $\text{mm}^2/\text{hr}$ . A sample with enough dots to produce a convenient ESR signal can be written in  $\sim 3$  hours.

Recently we have also demonstrated the fabrication of large-area arrays of uniform dots down to about 70 nm physical diameter without using ion-based etching. Only wet etches were used, which means that no extra damage was introduced (there could still be defects associated with exposing the Si and SiGe surfaces). Controlling the wet etching is difficult, since it is isotropic. However, by defining a somewhat larger dot in the resist, and carefully controlling the etch times, we can consistently make dots with diameters under 100nm. The ESR signals we see in the wet etched dots are essentially the same as those we find after RIE and a short wet etch. Thus, we conclude that RIE can probably be used. More recently, however, we have developed an etch recipe for SiGe to be used in an electron-cyclotron resonance (ECR) etcher, in which the energy of the ions impacting the surface can be reduced to a very low value. This etcher is normally used to pattern high-mobility GaAs/AlGaAs 2D electron devices, and produces very little damage. With the ECR etcher we do not find a damage signal after etching dots. The ESR spectra

from devices patterned with the ECR etcher are very similar to those from wet-etched devices, with the advantage that the ECR etches anisotropically and can readily pattern small quantum dots.

As the dots are made smaller, their energy levels will be pushed farther apart. However, even for small, 70 nm quantum dots, we must measure at low temperatures to avoid thermal excitation of the electrons to upper states. We have finished installing and testing a  $^3\text{He}$  system for measuring ESR at lower temperatures (our base temperature is about 350 mK). Our initial measurements do not show a large increase in  $T_2$  at this temperature. It is likely that the quantum dots are large enough that each contains several electrons, and that the interactions between the electrons are limiting the coherence. Structures which will give us greater control over the charge in a dot are being developed.

We have also measured spin resonance from a large-area Si MOSFET. Below the threshold for conduction, electrons are confined in shallow states associated with the fixed charges and disorder in the oxide – naturally occurring quantum dots. We find that mobile electrons (above threshold) have a  $T_2$  of about  $0.3\mu\text{s}$  at 5K, while the confined electrons have a  $T_2$  of over  $2\mu\text{s}$ . We have evidence that the spin coherence of the confined electrons becomes longer at lower temperatures, since then they will be better frozen into the confined states.

A major development we have recently made has been a study of dynamic decoupling for preserving the coherence of qubits. It seems that essentially all qubits suffer from decoherence from  $1/f$  (or more generally,  $1/f^\alpha$ ) noise at some level. Slow decoherence of this variety can, in principle, be reduced or eliminated with a dynamic decoupling sequence. There has been significant theoretical effort along these lines, but most of the theories have ignored the practical reality of imperfect controls (microwave pulses, in our case). For example, systematic errors in the pulse amplitude make sequences such as CPMG (Carr-Purcell-Meiboom-Gill) unsuitable, since they preserve one qubit state well,  $\frac{1}{2}(|0\rangle + |1\rangle)$ , but not another,  $\frac{1}{2}(|0\rangle + i|1\rangle)$ . Using donor-bound electrons for testing we have found that a commonly suggested sequence,  $\tau$ -X- $\tau$ -Z- $\tau$ -X- $\tau$ -Z (where the  $\tau$ 's represent free precession), is much better than CPMG, but it still differentiates between different initial states in a real system. However, we find that dynamic decoupling with the sequence,  $\tau$ -X- $\tau$ -Y- $\tau$ -X- $\tau$ -Y, not only preserves coherence, but we find no dependence on the initial state after hundreds of imperfect microwave pulses. These results could have important implications for error correction and avoidance.

## **Work led by Purdue and JPL (G. Klimeck and P. von Allmen)**

### **Accomplishments for 2006**

1. Valley splitting in tilted quantum wells: We have calculated the electronic structure in quantum wells with rough interfaces using our atomic-level model. We have shown that the valley splitting, which is one of the crucial electronic structure properties of a silicon quantum dot, is exactly zero when the roughness at the interface is arranged periodically. These results have been submitted for publication.
2. Magnetic effect on valley splitting in tilted quantum wells: we have calculated the valley splitting in a quantum well with rough interfaces as a function of the strength of a magnetic field applied perpendicularly to the quantum well. We have obtained an increase of the valley splitting as the amplitude of the magnetic field increases, as has been observed experimentally by the QCCM team and other researchers previously. The functional dependence is however not the same as in the experiment, where a linear dependence was observed. These results were submitted for publication.
3. Valley splitting in quantum wires: We have calculated the valley splitting in a silicon quantum wire, which is a structure where the electrons are confined in two directions. The confinement is achieved by using two electronic gates at the surface of the device to compel the electrons in a quantum well to reside between the two gates. The electronic structure was obtained by self-consistently solving the TB equations and the electrostatic Poisson equation. We have obtained that the confinement increases the valley splitting as was observed experimentally by the QCCM team.
4. Exchange interaction in a quantum well: We have performed preliminary calculations of the exchange interaction between the electrons in a quantum well. The exchange interaction results from the Pauli exclusion principle stating that two electrons cannot reside in the same electronic energy state. We have obtained that the exchange interaction increases the valley splitting in presence of a magnetic field as was previously predicted with models that do not use an atomic-level description.

### **Accomplishments for 2007**

1. Tight-binding parameters for atomistic modeling of SiGe: We have used the Virtual Crystal Approximation to describe the SiGe alloy material. In this approximation, the alloy is described by

“average” parameters that are obtained from an interpolation process using the Si and Ge parameters. We have verified that the energy band edges are accurately described within the experimental error of the data available in the literature.

2. Effect of interface disorder on valley splitting in SiGe quantum wells and quantum wires: As a general statement, disorder destroys the translation symmetry of the steps in quantum wells grown on tilted substrates and therefore increases the valley splitting. Recent results in the literature show that the dominant effect of disorder stems from the alloy disorder in the quantum well barriers. The irregularity along the steps plays a minor role. We have therefore only included disorder due to the alloy, and more specifically the disorder induced by the atomic-level intermixing (over 1 atomic monolayer) between the barrier and well materials. We have shown that the valley splitting is extremely sensitive to the degree of disorder at the interface. This result is in agreement with the observation that the effect of valley splitting is dominated by a potential strongly localized at the interface (see theoretical work from the University of Wisconsin).

3. Occupation of confined levels in SiGe quantum wells and quantum wires as a function of electric field: A key aspect of computing the electronic states for electrostatically defined quantum dots is to determine the number of occupied levels. This is a complex problem that involves among others the escape rate from the quantum-confined structure for a given applied bias on the gates. The escape rate is obtained from the overlap of the confined wavefunction with the region with large electric field toward the bottom gate.

4. Self-consistent solution of 3D Poisson equation and atomistic model: We made progress toward completing a multi-scale simulation tool by integrating a 3D Poisson equation solver with the tight-binding description of the material. Adaptive Delaunay meshing, Dirichlet tessellation and a finite volume Poisson equation solver were implemented in the atomistic modeling package. Self-consistent calculations for realistic 3D gates and an atomistic description of the materials are currently being tested.

#### **Accomplishments for 2008**

1. Electronic states for realistic electrode structures: The top electrodes create a region in the 2-dimensional electron gas, where the electron potential energy is lower than in the rest of the quantum well. The shape of this potential well, and hence the electronic structure of the confined states, is determined by

the self-consistent solution of the Poisson equation (giving the electrostatic potential) and the Schrödinger equation (giving the electronic wavefunctions and charge density). The size of the simulation domain in the plane of the quantum well for a realistic solution of the Poisson equation is about  $4 \text{ nm}^2$ . The size of the domain in the direction perpendicular to the QW is about 0.1 nm. If the entire domain were to be described with an atomic-level model, the total number of atoms in the system would be about 25 billion, far beyond current simulation capabilities. It is therefore clear that the simulation package has to include continuum models for the materials alongside with atomic level approaches. In the past year, we have developed and integrated a 3-D finite element solver of the Poisson equation with a hierarchy of 4 levels for the description of the electrons: 1) A semiclassical model where the electrons are described by a density field that is a simple function of the electrostatic potential, 2) An effective mass approximation, where the electrons are described by a Schrödinger equation and a longitudinal and a transverse effective mass, 3) A tight-binding model that was parameterized to reproduce certain bulk properties, and 4) A density functional method that is a parameter free approach. Fully integrated electronic structures are now being obtained.

2. Toward simulating decoherence in realistic structures: One of the main decoherence mechanisms for spin qubits in Si QD's is the interaction with phonons. We have computed the electron-phonon interaction in the context of electrical conductivity calculations for nanowires. We use a realistic phonon distribution obtained with a sophisticated valence force field model and we calculate the electron-phonon coupling within the frozen phonon approximation that takes into account the anharmonicity of the ionic vibrations.

3. Temporal evolution of qubit states: One of the goals of this work is to simulation a qubit operation using a realistic model of the device. We implemented a density matrix solver that takes as input the electronic states and the coupling matrix elements with an electromagnetic field, from our atomic-level description of the materials. As an example application, we have calculated the non-linear optical response for a C60 buckyball.



4. We evaluated valley splitting on a (111)-oriented silicon wafer. In this geometry, a simple 6-fold valley degeneracy is expected. Experimentally, however, 2-fold and 4-fold degeneracies are observed. To explain this behavior, we performed atomistic calculations on a slanted wafer to determine the eigenstates. Our findings show that the wafer slant is responsible for the experimentally observed splitting. This work is un-published and will be submitted shortly.

5. We have also performed numerical calculations to analyze the valley splitting in realistic (finite) confinement potentials. Previously, we have reported on the importance of the details of the confinement potentials in SiGe/Si/SiGe quantum wells. In particular, the  $2^\circ$  interfacial tilt and the atomistic alloy disorder were found to be critical. In the past year, we have combined numerical and analytical techniques to show that the valley splitting is not only a strong function of quantum well width, but also of barrier height and can even lead to parity changes in the split valley states.

## Bibliography

1. Loss, D. and D.P. DiVincenzo, *Quantum computation with quantum dots*. Phys. Rev. A, 1998. **57**(1): p. 120-126.
2. Friesen, M., et al., *Practical design and simulation of silicon-based quantum-dot qubits*. Phys Rev B, 2003. **67**: p. 121301.
3. Eriksson, M.A., et al., *Spin Based Quantum Dot Quantum Computing in Silicon*. Quantum Information Processing, 2004. **3**: p. 133.
4. DiVincenzo, D.P., et al., *Universal quantum computation with the exchange interaction*. Nature, 2000. **408**(6810): p. 339.
5. Simmons, C.B., et al., *Single-electron quantum dot in Si/SiGe with integrated charge measurement*. Applied Physics Letters, 2007. **91**: p. 213103.
6. Petta, J.R., et al., *Coherent manipulation of coupled electron spins in semiconductor quantum dots*. Science, 2005. **309**: p. 2180-2184.
7. Koppens, F.H.L., et al., *Driven coherent oscillations of a single electron spin in a quantum dot*. Nature, 2006. **442**: p. 766-771.
8. Shaji, N., et al., *Spin blockade and lifetime-enhanced transport in a few-electron Si/SiGe double quantum dot*. Nat Phys, 2008. **4**(7): p. 540.
9. Goswami, S., et al., *Controllable valley splitting in silicon quantum devices*, in *Nat Phys*. 2007. p. 41-45.
10. Friesen, M., M.A. Eriksson, and S.N. Coppersmith, *Magnetic field dependence of valley splitting in realistic Si/SiGe quantum wells*, in *Appl Phys Lett*. 2006. p. 202106.